ACCOUNTS of chemical research

Article

pubs.acs.org/accounts

Two-Dimensional Colloidal Metal Chalcogenides Semiconductors: Synthesis, Spectroscopy, and Applications

Published as part of the Accounts of Chemical Research special issue "2D Nanomaterials beyond Graphene".

Emmanuel Lhuillier,[†] Silvia Pedetti,[†,‡] Sandrine Ithurria,[‡] Brice Nadal,[†] Hadrien Heuclin,[†] and Benoit Dubertret*[,‡]

[†]Nexdot, 10 rue Vauquelin, 75005 Paris, France

[‡]Laboratoire de Physique et d'Etude des Matériaux, ESPCI-ParisTech, PSL Research University, Sorbonne Université UPMC Univ Paris 06, CNRS, 10 rue Vauquelin 75005 Paris, France

CONSPECTUS: Semiconductors are at the basis of electronics. Up to now, most devices that contain semiconductors use materials obtained from a top down approach with semiconductors grown by molecular beam epitaxy or chemical vapor deposition. Colloidal semiconductor nanoparticles have been synthesized for more than 30 years now, and their synthesis is becoming mature enough that these nanoparticles have started to be incorporated into devices. An important development that recently took place in the field of colloidal quantum dots is the synthesis of two-dimensional (2D) semiconductor nanoplatelets that appear as free-standing nanosheets. These 2D colloidal systems are the newborn in the family of shaped-controlled nanoparticles that started with spheres, was extended with rods and wires, continued with tetrapods, and now ends with platelets.

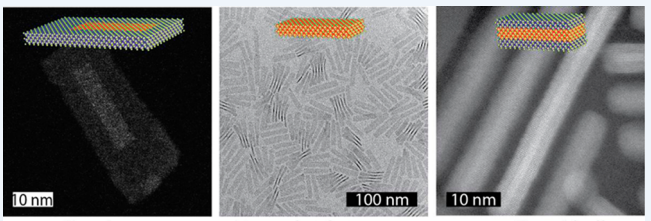

From a physical point of view, these objects bring 1D-confined particles into the colloidal family. It is a notable addition, since these platelets can have a thickness that is controlled with atomic precision, so that no inhomogeneous broadening is observed. Because they have two large free interfaces, mirror charges play an important role, and the binding energy of the exciton is extremely large. These two effects almost perfectly compensate each other, it results in particles with unique spectroscopic properties such as fast fluorescent lifetimes and extreme color purity (narrow full width at half-maximum of their emission spectra). These nanoplatelets with extremely large confinement but very simple and well-defined chemistry are model systems to check and further develop, notably with the incorporation in the models of the organic/inorganic interface, various theoretical approaches used for colloidal particles.

From a chemical point of view, these colloidal particles are a model system to study the role of ligands since they have precisely defined facets. In addition, the synthesis of these highly anisotropic objects triggered new research to understand at a mechanistic level how this strong anisotropy could be generated. Luckily, some of the chemical know-how built with the spherical and rod-shaped particles is being transferred, with some adaptation, to 2D systems, so that 2D core/shell and core/crown heterostructures have recently been introduced. These objects are very interesting because they suggest that multiple quantum wells could be grown in solution. From the application point of view, 2D colloidal nanoplatelets offer interesting perspectives when color purity, charge conductivity, or field tunable absorption are required. In this Account, we review the chemical synthesis, the physical properties, and the applications of colloidal semiconductor nanoplatelets with an emphasis on the zinc-blende nanoplatelets that were developed more specifically in our group.

1. INTRODUCTION

The discovery of the size dependent optical properties of semiconductor colloidal quantum dots (CQDs) is about 30 years old, and the community of scientists working in the field has recently celebrated this event at ESPCI.[1] Although the field started in the early 1980s, with the pioneering work of Ekimov,[2] Efros,[3] and Brus,[4] it is the first synthesis of spherical colloidal nanocrystals (NCs) with a precise control of the size dispersion (~5%) in 1993[5] in the group of Bawendi that established the solution growth of NCs as a very promising route for the synthesis and the applications of colloidal QDs. Since then, the synthesis of CQDs has been extended to a large variety of materials,[6] of compositions,[7] and of morphologies.[8] The control of the shape, spheres, rods,[9] wires,[10] or plates,[11] of CQDs is interesting since it brings a unique way to tune the confinement, 3D, 2D, or 1D, of the charge carriers and as a consequence their density of states. Among the different shapes, nanoplatelets (NPLs) are of particular interest because it has been shown that their thickness can be controlled with atomic precision. Their large planar facets can be precisely

Special Issue: 2D Nanomaterials beyond Graphene

Received: September 2, 2014
Published: January 2, 2015

DOI: 10.1021/ar500326c
Acc. Chem. Res. 2015, 48, 22−30

defined chemically as is the case for other 2D systems such as graphene or 2D dichalcogenide[12] materials that are also detailed in this special issue. As a consequence, nanoplatelets can serve as a model system to better understand the effect of surface chemistry, of composition, and of confinement in semiconductor systems.

Several reviews on the synthesis of 2D colloidal systems have already been written,[13,14] and another one from the group of W. Buhro is in this special issue. The reader is referred to these reviews for additional information. In this Account, we detail the growth mechanisms of colloidal NPLs, and we present the possibility to obtain 2D heterostructures such as core/shell and core/crown NPLs, either by colloidal synthesis or using cation exchange. We review the unique optical properties of these 2D structures, as well as their use in devices such as light emitting diodes, field effect transistors, and photodetectors.

2. MATERIALS

2.1. Growth Mechanisms of 2D Nanoplatelets

Two-dimensional metal chalcogenide semiconductor nanoplatelets can be synthesized in three different crystal structures: zinc blende, wurtzite and rock salt. We describe rapidly the synthesis of these three families of NPLs, with an emphasis on the zinc blende NPLs that were developed mainly in our group.

2.1.1. Wurtzite NPLs. In 2006, Hyeon and co-workers reported the synthesis of CdSe nanoribbons[15] (Figure 1e) that were obtained thanks to a lamellar-like template growth induced by the dissolution of cadmium chloride in an amine in which a selenium precursor is slowly reduced. Soon after, CdS[16] and CdTe[17] nanoribbons were synthesized using similar syntheses. The growth mechanism of these wurtzite 2D crystals has been investigated by the teams of Hyeon[18,19] and Buhro[20−22] and was shown to proceed through the templated assembly of magic size clusters such as $CdSe_{13}$ or $CdSe_{34}$ as proposed in path 1 of Figure 1d. ZnS nanoplatelets (Figure 1f) can also be grown by this method, even if the presence of clusters as building blocks has not yet been proven. Wurtzite NPLs are generally synthesized at relatively low temperature (<100 °C), using cadmium acetate or halide precursors in long chain amine solvent. These NPLs have large surfaces that are formed of a mixture of anions and cations.

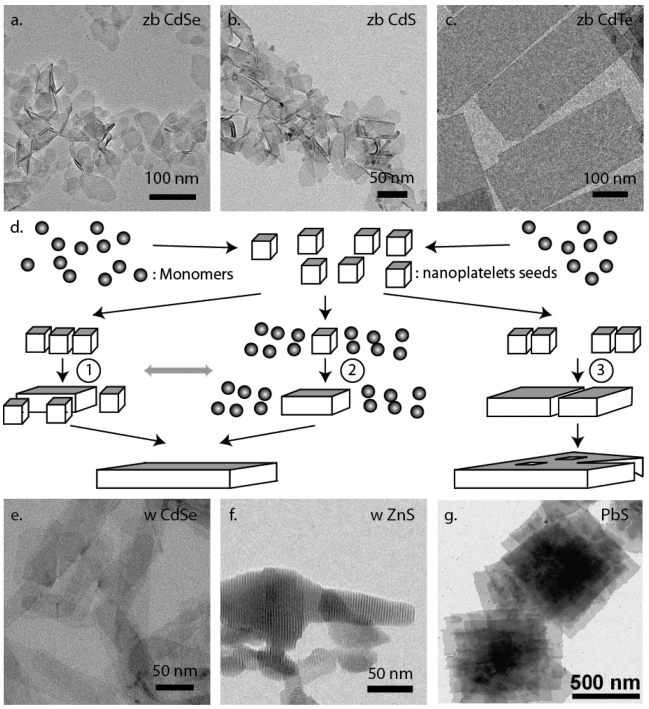

Figure 1. TEM images of zinc blende CdSe (a), CdS (b), CdTe (c), wurtzite CdSe (e), and ZnS (f) and rock salt PbS (g) NPLs. From ref 23. Reprinted with permission from AAAS. (d) Scheme of the different paths for the growth of nanoplatelets. Adapted with permission from ref 24. Copyright 2011 American Chemical Society.

2.1.2. Zinc Blende NPLs. In 2008, our group reported the first synthesis of zinc blende CdSe nanoplatelets (Figure 1a) with different thicknesses that were controlled with atomic precision.[11] In 2011, the syntheses of zinc blende NPLs were extended to CdS and CdTe[25] (Figure 1b,c). In these syntheses, the anisotropy is obtained by mixing a short chain carboxylic acid with a cadmium carboxylate with a longer aliphatic chain so that the cadmium precursors can be assimilated to $Cd(R_1COO)(R_2COO)$ with R_1 either CH_3 or C_2H_5 and R_2 an aliphatic chain with more than 10 carbons. The anionic precursor can either be complexed to trioctyl phosphate (TOP) or mixed as a powder in a solvent, usually octadecene. The growth of these nanoplatelets is performed at higher temperature (120−250 °C) compared to the temperature of the growth of wurtzite NPL. The formation of zinc-blende nanoplatelets starts with well-defined seeds with spectral characteristics comparable to so-called "magic sized clusters".[24] These seeds have two cation-rich facets that are poisoned by ligands and that can extend laterally through continuous reaction of precursors, as presented in path 2, Figure 1d. This lateral extension can be continuously followed by monitoring the red shift of the excitonic peaks up to the point where the lateral dimensions of these "quantum wells" are larger than 2 times the 2D Bohr radius.[26] Below these dimensions, the exciton experiences a 3D confinement that increases the excitonic energy transition. For larger dimensions, the exciton is purely 1D confined, and the full width at half-maximum (fwhm) of the NPL photoluminescence is narrowest (close to k_BT). The lateral extension of NPLs can be performed with continuous injection of precursors to reach lateral dimensions of a few hundred nanometers for CdSe[27] and CdTe[28] NPLs. Today, one can control not only the lateral size and the composition of the NPLs but also their thickness by varying the reaction conditions.[25] For a given synthesis, the later the acetate salt is introduced the thicker the NPLs. Similarly, for CdS NPLs, low temperature and shorter aliphatic chains favor thinner NPLs.[29]

2.1.3. Rock Salt NPLs. Apart from zinc-blende and wurtzite NPLs, Weller and co-workers have synthesized in 2010[23] lead sulfide nanoplatelets with a rock salt crystal structure, thanks to the oriented attachment of lead sulfide nanocrystals. The introduction of a chloride compound that binds to Pb altered the nucleation and growth of PbS and led to small nanocrystals (<3 nm), which exhibit the highly reactive (110) facets necessary for oriented attachment (see path 3 in Figure 1d,g).

2.2. Nanoplatelet Heterostructures

2.2.1. Core/Shell. As for spherical QDs, the possibility to enrich the landscape of 2D nanocrystals with heterostructures such as core/shell (Figure 2a) is fascinating. Indeed, deposition of a shell can enhance the optical properties, for example, higher quantum yield and better photostability,[7,30,31] than core-only NCs. While several methods exist to grow shells on QDs

DOI: 10.1021/ar500326c
Acc. Chem. Res. 2015, 48, 22−30

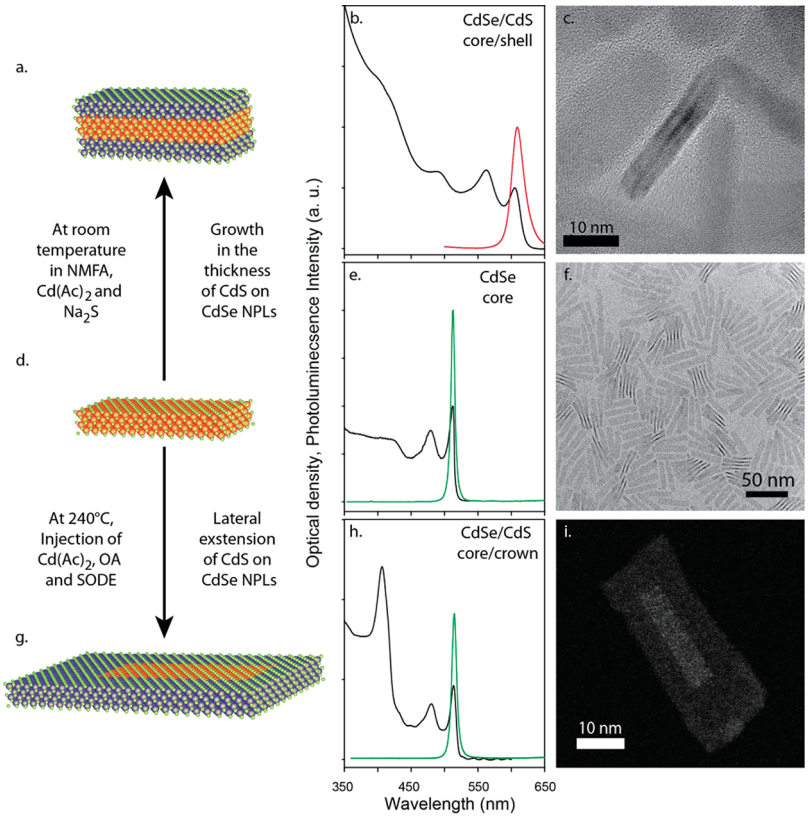

Figure 2. (a) Scheme of core/shell CdSe/CdS NPLs with its absorption and PL spectra (b) and its TEM image (c). (d, e, f) Same set of data for core only NPL. (g, h, i) Same set of data for CdSe/CdS core/crown NPLs.

and rods,[32,33] only two techniques have been developed so far to obtain 2D core/shell NPLs such as CdSe/CdS NPLs (Figure 2a).[34,35] The first method, named colloidal atomic layer deposition (*c*-ALD), allows fine control of the shell thickness and its composition. This method consists of an alternate deposition of anionic and cationic monolayers. As mentioned earlier, zinc-blende NPLs have two Cd rich facets passivated with oleate chains. These Cd rich facets can be covered with a sulfide layer using TMS_2S, $(NH_4)_2S$, Na_2S, or NaSH.[36] This sulfide coverage comes with a ligand exchange and a transfer of the NPLs from a nonpolar to a polar phase.[37] The next cationic layer is grown with the reaction of NPLs with a cadmium salt. At each step of the reaction, the excess of precursors can be removed using precipitation. The second method to make core/shell NPLs is a "one pot" method based on the *in situ* generation of hydrogen sulfide by the reaction of thioacetamide with octylamine.[38] A cadmium source is added, and the reaction is allowed run for a few hours. Both methods can be successfully applied on different thicknesses and lateral sizes. The absorption spectrum of core/shell NPLs shows two excitonic peaks (Figure 2b), red-shifted compared with the cores, due to the electron delocalization over the entire thickness of the NPL. Such core/shell NPLs exhibit high QY, up to 80%.[39]

2.2.2. Core Crown. Another type of 2D heterostructures has been recently developed that allows the lateral extension of the NPLs. The group of Artemyev and our group have reported the synthesis of CdSe/CdS core/crown NPLs (Figure 2g,h,i).[40,41] As for core NPLs, the lateral extension is achieved by using a combination of long chain and short chain carboxylate ligands (typically an acetate and an oleate), as it has been used for the lateral extension of CdSe NPLs into CdSe nanosheets.[27] The resulting crown has the same thickness as the starting NPL. Contrary to core/shell structures, almost no red shift of the emission peak is observed during the growth of the CdS crown. This absence of red shift is explained by the strong (~300 meV) binding energy of the exciton,[42] which is greatly enhanced compared with spherical objects. Because of this large binding energy, the Bohr radius of the exciton is very small (~1−2 nm), and there is no lateral confinement in the NPLs. Consequently, lateral extension does not produce any PL emission red shift. In these heterostructures, both core and crown sizes can be controlled. These new objects exhibit enhanced photoluminescence compared with the starting core NPLs (up to 60% QY) as well as a very high absorption cross section in the CdS region (Figure 2h). Spectroscopic studies showed that these objects can act as exciton funnels where the excitons are collected in the CdS crown and rapidly and efficiently transferred to the CdSe core where the recombination occurs. Recently the growth of CdTe crown with a type II band alignment was also proposed.[43]

2.3. Expanding the Range of Available Material through Cation Exchange

Recently, cation exchange reactions have been developed as an alternative approach to obtain materials that are difficult to synthesize by direct methods. Many groups have demonstrated the potential of this method on spherical or rod-shaped core[44−46] or core/shell[47] nanoparticles. Regarding 2D nanostructures, Moreels et al. have published the preparation of CdTe nanodisks from Cu_2Te by cation exchange.[48] The group of Lee has prepared ZnS/Ag_2S heterostructures from ZnS nanosheets.[49] Bouet et al. have studied cation exchange on

DOI: 10.1021/ar500326c
Acc. Chem. Res. 2015, 48, 22−30

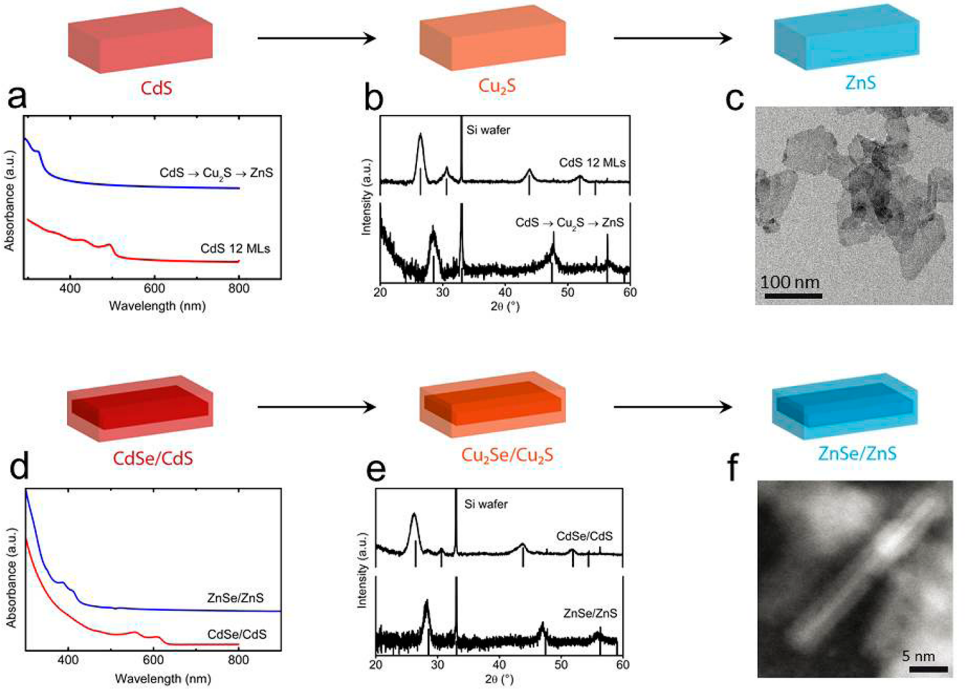

Figure 3. Cation exchange on CdS: (a) Absorption spectra and (b) X-ray powder diffraction patterns of CdS NPLs and Zn exchanged NPLs and (c) TEM image of Zn exchanged NPLs. Cation exchange on CdSe/CdS: (d) absorption spectra and (e) X-ray powder diffraction patterns of CdSe/CdS NPLs and Zn exchanged NPLs and (f) TEM image of Zn exchanged NPLs. Adapted with permission from ref 50. Copyright 2014 American Chemical Society.

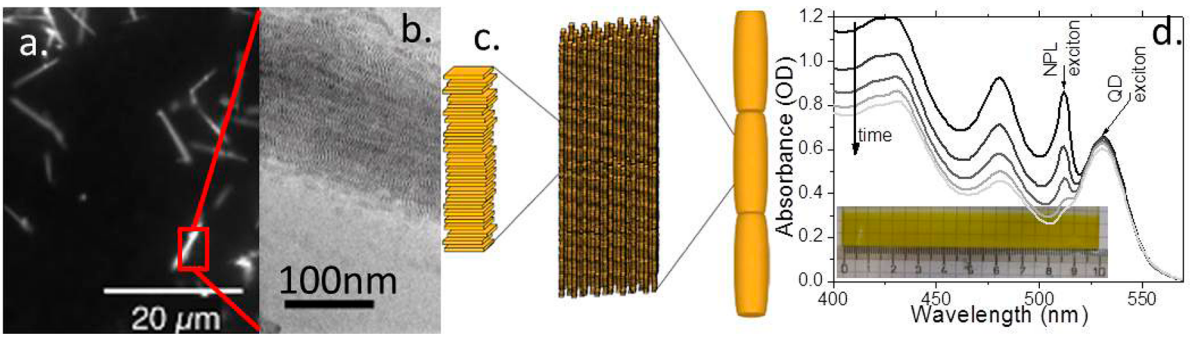

Figure 4. (a) Optical microscopy and (b) TEM images of CdSe nanoplatelet superlattices. (c) Scheme representing the hierarchical structure of the superlattices. Adapted with permission from ref 59. Copyright 2014 American Chemical Society. (d) Absorption spectra of a mixture made of QDs and NPLs at different times during the electrophoresis of the mixture. The inset is a film of NPLs deposited using electrophoresis. The scale is in centimeters.

cadmium based 2D shaped nanoparticles.[50] Starting from CdS or CdSe/CdS NPLs, ZnS (Figure 3a–c) and PbS core or ZnSe/ZnS (Figure 3d–f) and PbSe/PbS core/shell structures were obtained. During the steps of cation exchange, the NPL shape is conserved as long as the thickness of the NPL is larger than 1.8 nm (Figure 3c,f). Moreover, after exchange, zinc-based nanostructures exhibit a zinc-blende structure, identical to the initial nanoparticles, whereas, with lead, the final structure turns to rock-salt. Finally when exchanging, cations diffuse uniformly from the largest surfaces through the NPLs. Recently, the group of Manna showed that copper selenide–sulfide nanoplatelets could be transformed without morphological change into copper tin zinc selenide–sulfide NPLs.[51]

2.4. Other

2.4.1. Self-Assembly. Self-assembly of nanoparticles into large and ordered structures is motivated by the idea to build at the nanoscale engineered hybrids.[52,53] However, the real benefit is correlated to the fine control of the three-dimensional organization of the nanoparticles. Few examples concerning the self-assembly of 2D anisotropic nano-objects exist in the literature. For instance, Cu_2S nanodisks[54] or nanoplates[55,56] can form a columnar assembly in solution thanks to additives or by slow evaporation of the solvent. Moreover, Murray and co-workers have used the interfaces of two liquids to self-assemble lanthanide fluoride nanoplatelets into long ranged superlattices.[57,58] For II–VI materials, Abécassis et al. have reported the self-assembly of CdSe nanoplatelets into micrometer long needles with very hierarchized structure[59] (Figure 4a,b,c). These superstructures are obtained spontaneously upon addition of a nonsolvent to colloidal solutions and are formed of about 10^6 nanoplatelets. Interestingly, these superstructures emit strongly polarized light, a property that could be exploited in some optoelectronic devices.

DOI: 10.1021/ar500326c
Acc. Chem. Res. 2015, 48, 22–30

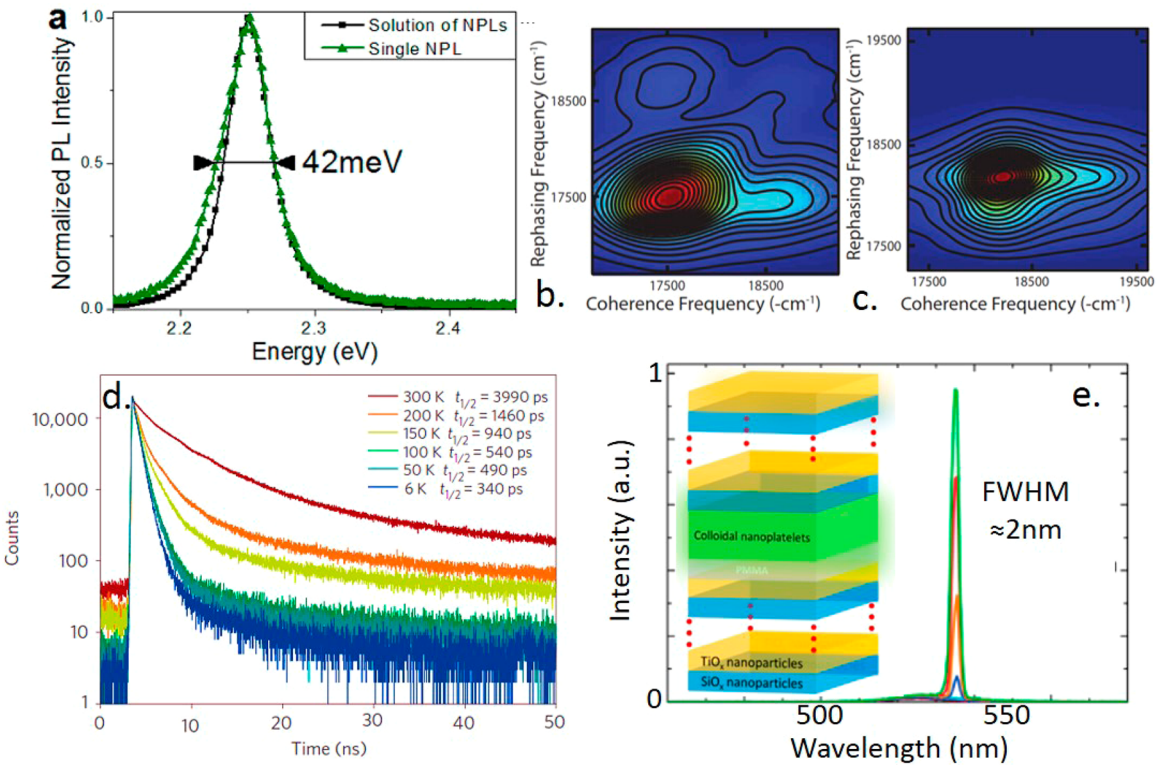

Figure 5. (a) PL spectrum of a single CdSe NPL and of an assembly of them at room temperature. Reprinted with permission from ref 61. Copyright 2012 American Chemical Society. Two-dimensional electronic spectrum of colloidal spherical QDs (b) and NPLs (c). Reprinted with permission from ref 62. Copyright 2013 AIP Publishing LLC. (d) Time resolved PL spectra of CdSe NPLs at different temperature. Reprinted by permission from Macmillan Publishers Ltd., *Nature Materials*, from ref 25, copyright 2011. (e) Lasing signal of core−shell NPLs integrated between two colloidally prepared Bragg mirrors. Adapted with permission from ref 63. Copyright 2014 American Chemical Society.

2.4.2. Electrophoretic Manipulation of NPLs. Strategies to clean a large amount of material had to be developed to increase the production of these NPLs. Lhuillier et al. reported an electrophoretic procedure to separate NPLs from other byproducts, such as spherical QDs, during the synthesis.[60] The electrophoretic separation relies on the strong difference of electrophoretic mobility between the two species (ratio of 400). NPLs can be extracted from a QDs/NPLs mixture with high efficiency (>90%) within a 3 min time scale (Figure 4d). The procedure can also be used for the large scale deposition (>10 cm) of NPL films (Figure 4d, inset).

3. SPECTROSCOPY

3.1. Narrow PL and Fast Lifetime

Colloidal NPLs exhibit three striking features compared with QDs: a narrow optical feature, fast photoluminescence (PL) lifetime, and almost no Stoke's shift.[61] At room temperature, the ensemble emission spectrum is almost the same as at the single particle one (Figure 5a). The fwhm at RT typically ranges from 7 to 10 nm, corresponding to a line width between $1k_bT$ and $2k_bT$. Contrary to QDs, NPLs present a thickness control at the atomic scale leading to a PL without inhomogeneous broadening. This observation has been confirmed using 2D spectroscopy (Figure 5b,c).[62] Compared to 0D and 1D nanorods, NPLs present narrower PL signal along the diagonal (homogeneous broadening) and perpendicular to the diagonal (inhomogeneous broadening).

3.2. Nanoplatelet Band Structure

One of the main promises of NPLs is their 2D character. The band structure of NPLs has been modeled using different approaches: infinite well approximation,[11] k·p modeling,[25] Hartree renormalized k·p method,[64] and tight binding.[42] These different models all attribute the first two excitonic features to the heavy hole to electron and light hole to electron transitions (Figure 2e).

Moreover, the facets of these platelets are capped with organic ligands, and the platelets are typically surrounded by solvents or by air. This means that carrier confinement and exciton binding energies are much stronger in colloidal nanoplatelets than in epitaxial QWs,[42,64] which are buried in a crystal of a second semiconductor material. The strongly bound character of the exciton in NPLs was then confirmed using time-resolved spectroscopy method.[65] One of the consequences of this is an enhanced oscillator strength.[25]

Compared to 0D QDs, the PL lifetime is much faster in NPLs (Figure 5d).[25,66] It is of a few nanoseconds at room temperature going down to 300 ps at 4 K. The dynamic of the exciton in the NPLs has also been tested using transient absorption. Pelton et al. concluded that the exciton indeed behaves as a 2D system. While optically charging the system, the authors observe first a bleach of the interband transition as well as the appearance of a new peak in the near-infrared[67] very likely related to some intraband feature. The role of the phonon into NPL is not yet completely clear since both fast[67] and slow[64] coupling to LO phonon has been claimed. Another striking feature related to the assembly of nanoplatelets is the appearance of a second PL peak attributed to the phonon

DOI: 10.1021/ar500326c
Acc. Chem. Res. 2015, 48, 22−30

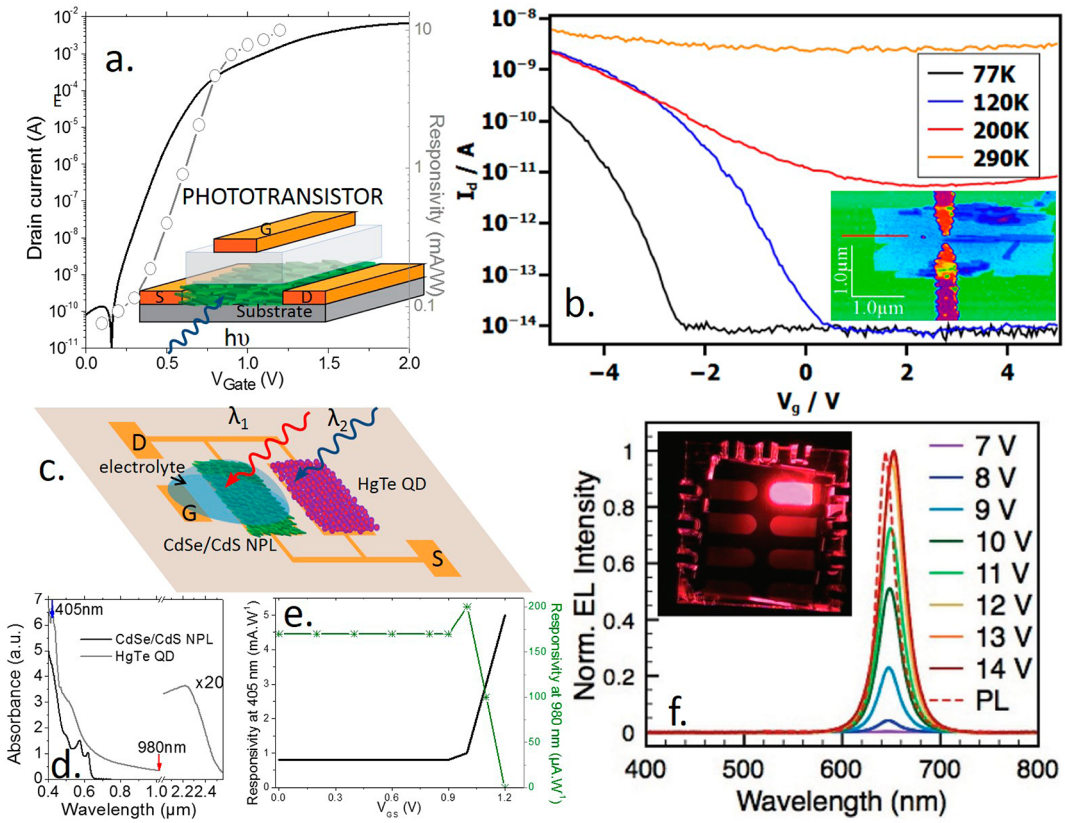

Figure 6. (a) Transfer curve (drain current vs gate bias) for a film of CdSe/CdS NPLs gated with ion gel polymer. VDS is set at 0.5 V, and measurements are made at room temperature in air. The inset is a scheme of the device. (b) Transfer curve for a transistor made of a single PbS NPL. The inset is an AFM image of the device. Reprinted with permission from ref 75. Copyright 2012 AIP Publishing LLC. (c) Scheme of a bicolor detector made of a gated film of CdSe/CdS NPLs and HgTe CQDs. (d) Absorption spectrum for CdSe/CdS NPLs and for HgTe CQDs. (e) Responsivity at 405 and 980 nm as a function of gate bias for the device of part c. Adapted from ref 76. Copyright 2014 American Chemical Society. (f) Electroluminescence spectra of CdSe/CdS NPLs under different biases. The inset is a picture of the device under operation. Adapted from ref 77. Copyright 2013 WILEY-VCH Verlag GmbH.

replica due to the higher phonon coupling in strongly packed NPL assemblies.[68]

3.3. ASE and Lasing

The fast PL lifetime is extremely interesting from a light-emission perspective. In addition to the integration of NPLs into LED, which is discussed in the next section, NPLs appear as candidates for stimulated emission and lasing. She et al. and Guzelturk et al., respectively, reported amplified spontaneous emission (ASE) properties from CdSe/CdS core/shell[69] and core/crown NPLs.[63] In both cases, a significant decrease of the power threshold for amplified stimulated emission compared with QDs is observed (6 μJ·cm^{-2} in the core/shell geometry) and the gain measured are higher (~600 cm^{-1}, at least 4-fold the one of QDs). This result also stands when performing two photons pumping.[63] Reference 63 takes advantages of this large gain to integrate NPLs between two Bragg mirrors (Figure 5e, inset) and report a two photons pumped laser with a fwhm of 2 nm and a threshold of 2.5 mJ·cm^{-2}.

4. DEVICES

Integration of NPLs into optoelectronic devices[70] has been less studied than their spectroscopic properties. Nevertheless, NPLs offer some interesting perspectives for transport. In a film of CQDs, the transport is a hopping process where the carrier has to tunnel through the interparticle medium (i.e., the ligands). This process is responsible for the overall low mobility of CQD solid (10^{-6} cm^2 V^{-1} s^{-1} with long ligands at the end of the synthesis to 1−10 cm^2 V^{-1} s^{-1} while using ionic[71−73] or metal chalcogenides ligands[37]). Thanks to their large lateral size, the number of hopping processes requested to reach the electrodes is reduced while switching from QDs to NPLs. The transport in films of NPLs has been probed in a transistor configuration.[74] The gating is ensured using ion gel electrolyte. The film made of CdSe or CdSe/CdS NPLs presents a n-type character, while the CdTe NPLs are p-type. Our group obtained record on/off ratio above 10^8 on CdSe/CdS, while the subthreshold slope is 80 mV/decade (Figure 6a).

A key advantage of NPLs compared to 0D structures is their potentially stronger compatibility with usual technological processes thanks to their large lateral size. While for CQDs, the connection of the particles at the single particle remains tricky,[78] NPLs are the right candidate to connect a single particle using a top down approach. It consequently becomes reasonable to connect a single particle using an e-beam lithography process, as commonly done for graphene sheets. Klinke's group reported a transistor and detector obtained by the connection of a single PbS nanosheet (Figure 6b).[75] Almost no gate effect is achieved at room temperature, consistent with the narrow band gap nature of the PbS nanosheets. On the other hand, large current modulations (on/off ratio of 10^5) are obtained at low temperature. One of the key advantages of these micrometer scale nanosheets compared with 0D objects is

DOI: 10.1021/ar500326c
Acc. Chem. Res. 2015, 48, 22−30

their large absorption cross section, which allows a large current modulation under illumination even on a single particle.

Films of NPLs also present photoconductive behavior but with poor photoresponse (10 $\mu A \cdot W^{-1}$). One of the possible reasons for such low responsivity is the strong exciton binding energy of NPLs. Typically, for 10 V applied over 10 μm spaced electrodes the potential drop per NPL is around tens of millielectronvolts, not enough to dissociate the electron/hole pair with a binding energy higher than 200 meV.[42,64] A possible way to enhance the photoresponse of the NPL film is to gate the film using ion gel electrolyte. By raising the Fermi level just below the conduction band, the trap states are filled and the photoactivated carriers can no longer get trapped. The gating leads to an increased photocarrier lifetime and finally to a rise of the photoresponse up to three decades (Figure 6a). This gated film of NPLs was also used to build the first bicolor detector[76] based only on colloidal nanocrystals (Figure 6c). The device relies on two materials: HgTe CQDs with a response up to mid-infrared and CdSe/CdS NPLs with a photoresponse in the visible only (Figure 6d). By switching the gate bias, the authors demonstrated that the spectral range of one material or the other can be activated (Figure 6e).

Another interesting aspect of nanoplatelets for optoelectronic devices is the fine control of their optical features. The narrow PL line width of the CdSe cores (fwhm $\approx$ 10 nm) and CdSe/CdS core/shells (fwhm $\approx$ 20 nm) can be used to build LEDs with narrow electroluminescence emission. Such narrowness paves the way for LED devices with an improved color gamut. CdSe/CdZnS NPLs have been integrated in a p−n junction where ZnO nanocrystals are used as the n-layer and PEDOT−PVK as the hole-transport layer,[77] see Figure 6f. As the bias of the sample is increased, a red shift of the transition is observed attributed to the Stark effect.[79]

5. CONCLUSION

In this Account, some of the recent results related to metal chalcogenide 2D colloidal nanoplatelets are discussed. Atomic control of the growth can be obtained thanks to a careful control of the ligands capping the different facets of a seed. Core/shell as well as core/crown heterostructures can be synthesized. The lack of inhomogeneous broadening allows PL features to be reached that are so far inaccessible to spherical QDs. Spectroscopic measurements have confirmed the 2D character of the NPLs from band structure and charge carrier dynamics points of view. NPLs appear as very promising candidates for lasing since very low power threshold has been reported. Integration of NPLs into devices has led to very promising performance for phototransistor and single particle electronics.

AUTHOR INFORMATION

Corresponding Author

*E-mail: benoit.dubertret@espci.fr.

Notes

The authors declare no competing financial interest.

Biographies

Emmanuel Lhuillier got his Ph.D. from Ecole Polytechnique for his work on transport in superlattices under the supervision of Emmanuel Rosencher. He moved to University of Chicago (Guyot-Sionnest's group) where he worked on infrared photodetection using colloidal nanocrystals. He finally joined Nexdot where he is in charge of optoelectronic devices development.

Silvia Pedetti is currently a Ph.D. student at the Laboratoire de Physique et d'Etude des Matériaux in Paris. She received her M.Sc. in organic chemistry from the Università La Sapienza in 2011. Her research focuses on the synthesis and characterization of two-dimensional nanocrystals.

Sandrine Ithurria was undergrade at ESPCI (Paris); she joined the Dubertret's group in 2007 for her Ph.D. where she developed the synthesis of the 2D nanoplatelets. In 2010, she joined Talapin's group at The University of Chicago for her postdoctoral fellowship, where she worked on low temperature growth of colloidal nanocrystals. Since 2012, she has been assistant professor at ESPCI.

Brice Nadal received his engineer's degree from CPE Lyon in 2006. He obtained his Ph.D. degree from the University Paris Sud in 2009. In 2011, he conducted postdoctoral research at ESPCI with Benoit Dubertret and Hervé Aubin. He is currently working at Nexdot. His interests include the synthesis, characterization, and mechanistic investigation of organic and inorganic materials.

Hadrien Heuclin did his undergraduate studies at Ecole Polytechnique. He then completed his Ph.D. under the supervision of Dr. Nicolas Mézailles in 2012. His research interests focused on the synthesis of transition metal carbene complexes. He joined Nexdot where his work addresses the synthesis and characterization of 2D materials.

Benoit Dubertret received his Ph.D. from the University of Strasbourg in 1998 and completed a postdoctoral fellowship at The Rockfeller University in the group of Albert Libchaber. He is a CNRS researcher, group leader of the quantum dot team in the LPEM laboratory at ESPCI. His team is a 25 person group with interest in nanoparticle synthesis, bio application, visible optical spectroscopy, and device application. He is married and has 7 children.

ACKNOWLEDGMENTS

The authors thank Xiang Zhen Xu for her help with TEM imaging. B.D. thanks Agence National de la Recherche for funding (Grants SNAP and QDOTICS). This work has been supported by the Région Ile-de-France in the framework of DIM Nano-K.

REFERENCES

(1) Rogach, A. Quantum Dots Still Shining Strong 30 Years On. *ACS Nano* **2014**, *8*, 6511−6512.
(2) Ekimov, A. I.; Onushchenko, A. A. Quantum Size Effect in 3-Dimensional Microscopic Semiconductor Crystals. *JETP Lett.* **1981**, *34*, 345−349.
(3) Efros, A. L.; Efros, A. L. Interband Absorption of Light in a Semiconductor Sphere. *Sov. Phys.-Semicond.* **1982**, *16*, 772−775.
(4) Brus, L. E. A Simple-Model for the Ionization-Potential, Electron-Affinity, and Aqueous Redox Potentials of Small Semiconductor Crystallites. *J. Chem. Phys.* **1983**, *79*, 5566−5571.
(5) Murray, C. B.; Norris, D. J.; Bawendi, M. G. Synthesis and Characterization of Nearly Monodisperse Cde (E = S, Se, Te) Semiconductor Nanocrystallites. *J. Am. Chem. Soc.* **1993**, *115*, 8706−8715.
(6) Michalet, X.; Pinaud, F. F.; Bentolila, L. A.; Tsay, J. M.; Doose, S.; Li, J. J.; Sundaresan, G.; Wu, A. M.; Gambhir, S. S.; Weiss, S. Quantum Dots for Live Cells, in Vivo Imaging, and Diagnostics. *Science* **2005**, *307*, 538−544.
(7) Reiss, P.; Protiere, M.; Li, L. Core/Shell Semiconductor Nanocrystals. *Small* **2009**, *5*, 154−168.

DOI: 10.1021/ar500326c
Acc. Chem. Res. 2015, 48, 22−30

(8) Yin, Y.; Alivisatos, A. P. Colloidal Nanocrystal Synthesis and the Organic-Inorganic Interface. *Nature* **2005**, *437*, 664−670.
(9) Peng, X. G.; Manna, L.; Yang, W. D.; Wickham, J.; Scher, E.; Kadavanich, A.; Alivisatos, A. P. Shape Control of CdSe Nanocrystals. *Nature* **2000**, *404*, 59−61.
(10) Yu, H.; Li, J. B.; Loomis, R. A.; Gibbons, P. C.; Wang, L. W.; Buhro, W. E. Cadmium Selenide Quantum Wires and the Transition from 3D to 2D Confinement. *J. Am. Chem. Soc.* **2003**, *125*, 16168−16169.
(11) Ithurria, S.; Dubertret, B. Quasi 2D Colloidal CdSe Platelets with Thicknesses Controlled at the Atomic Level. *J. Am. Chem. Soc.* **2008**, *130*, 16504−16505.
(12) Chhowalla, M.; Shin, H. S.; Eda, G.; Li, L. J.; Loh, K. P.; Zhang, H. The Chemistry of Two-Dimensional Layered Transition Metal Dichalcogenide Nanosheets. *Nat. Chem.* **2013**, *5*, 263−275.
(13) Bouet, C.; Tessier, M. D.; Ithurria, S.; Mahler, B.; Nadal, B.; Dubertret, B. Flat Colloidal Semiconductor Nanoplatelets. *Chem. Mater.* **2013**, *25*, 1262−1271.
(14) Yang, J.; Son, J. S.; Yu, J. H.; Joo, J.; Hyeon, T. Advances in the Colloidal Synthesis of Two-Dimensional Semiconductor Nanoribbons. *Chem. Mater.* **2013**, *25*, 1190−1198.
(15) Joo, J.; Son, J. S.; Kwon, S. G.; Yu, J. H.; Hyeon, T. Low-Temperature Solution-Phase Synthesis of Quantum Well Structured CdSe Nanoribbons. *J. Am. Chem. Soc.* **2006**, *128*, 5632−5633.
(16) Son, J. S.; Park, K.; Kwon, S. G.; Yang, J.; Choi, M. K.; Kim, J.; Yu, J. H.; Joo, J.; Hyeon, T. Dimension-Controlled Synthesis of CdS Nanocrystals: From 0D Quantum Dots to 2D Nanoplates. *Small* **2012**, *8*, 2394−2402.
(17) Son, J. S.; Yu, J. H.; Kwon, S. G.; Lee, J.; Joo, J.; Hyeon, T. Colloidal Synthesis of Ultrathin Two-Dimensional Semiconductor Nanocrystals. *Adv. Mater.* **2011**, *23*, 3214−3219.
(18) Yu, J. H.; Liu, X. Y.; Kweon, K. E.; Joo, J.; Park, J.; Ko, K. T.; Lee, D.; Shen, S. P.; Tivakornsasithorn, K.; Son, J. S.; Park, J. H.; Kim, Y. W.; Hwang, G. S.; Dobrowolska, M.; Furdyna, J. K.; Hyeon, T. Giant Zeeman splitting in nucleation-controlled doped CdSe:Mn2+ Quantum Nanoribbons. *Nat. Mater.* **2010**, *9*, 47−53.
(19) Son, J. S.; Wen, X. D.; Joo, J.; Chae, J.; Baek, S. I.; Park, K.; Kim, J. H.; An, K.; Yu, J. H.; Kwon, S. G.; Choi, S. H.; Wang, Z. W.; Kim, Y. W.; Kuk, Y.; Hoffmann, R.; Hyeon, T. Large-Scale Soft Colloidal Template Synthesis of 1.4 nm Thick CdSe Nanosheets. *Angew. Chem., Int. Ed.* **2009**, *48*, 6861−6864.
(20) Liu, Y. H.; Wang, F. D.; Wang, Y. Y.; Gibbons, P. C.; Buhro, W. E. Lamellar Assembly of Cadmium Selenide Nanoclusters into Quantum Belts. *J. Am. Chem. Soc.* **2011**, *133*, 17005−17013.
(21) Wang, Y. Y.; Liu, Y. H.; Zhang, Y.; Wang, F. D.; Kowalski, P. J.; Rohrs, H. W.; Loomis, R. A.; Gross, M. L.; Buhro, W. E. Isolation of the Magic-Size CdSe Nanoclusters (CdSe)13(n-octylamine)13 and (CdSe)13(oleylamine)13. *Angew. Chem., Int. Ed.* **2012**, *51*, 6154−6157.
(22) Wang, Y. Y.; Zhang, Y.; Wang, F. D.; Giblin, D. E.; Hoy, J.; Rohrs, H. W.; Loomis, R. A.; Buhro, W. E. The Magic-Size Nanocluster (CdSe)(34) as a Low-Temperature Nucleant for Cadmium Selenide Nanocrystals; Room-Temperature Growth of Crystalline Quantum Platelets. *Chem. Mater.* **2014**, *26*, 2233−2243.
(23) Schliehe, C.; Juarez, B. H.; Pelletier, M.; Jander, S.; Greshnykh, D.; Nagel, M.; Meyer, A.; Foerster, S.; Kornowski, A.; Klinke, C.; Weller, H. Ultrathin PbS Sheets by Two-Dimensional Oriented Attachment. *Science* **2010**, *329*, 550−553.
(24) Ithurria, S.; Bousquet, G.; Dubertret, B. Continuous Transition from 3D to 1D Confinement Observed during the Formation of CdSe Nanoplatelets. *J. Am. Chem. Soc.* **2011**, *133*, 3070−3077.
(25) Ithurria, S.; Tessier, M. D.; Mahler, B.; Lobo, R. P.; Dubertret, B.; Efros, A. L. Colloidal Nanoplatelets with Two-Dimensional Electronic Structure. *Nat. Mater.* **2011**, *10*, 936−941.
(26) Bastard, G.; Mendez, E. E.; Chang, L. L.; Esaki, L. Exciton Binding-Energy in Quantum Wells. *Phys. Rev. B* **1982**, *26*, 1974−1979.
(27) Bouet, C.; Mahler, B.; Nadal, B.; Abecassis, B.; Tessier, M. D.; Ithurria, S.; Xu, X. Z.; Dubertret, B. Two-Dimensional Growth of CdSe Nanocrystals, from Nanoplatelets to Nanosheets. *Chem. Mater.* **2013**, *25*, 639−645.
(28) Pedetti, S.; Nadal, B.; Lhuillier, E.; Mahler, B.; Bouet, C.; Abecassis, B.; Xu, X. Z.; Dubertret, B. Optimized Synthesis of CdTe Nanoplatelets and Photoresponse of CdTe Nanoplatelets Films. *Chem. Mater.* **2013**, *25*, 2455−2462.
(29) Li, Z.; Peng, X. G. Size/Shape-Controlled Synthesis of Colloidal CdSe Quantum Disks: Ligand and Temperature Effects. *J. Am. Chem. Soc.* **2011**, *133*, 6578−6586.
(30) Mahler, B.; Spinicelli, P.; Buil, S.; Quelin, X.; Hermier, J. P.; Dubertret, B. Towards Non-blinking Colloidal Quantum dots. *Nat. Mater.* **2008**, *7*, 659−664.
(31) Hines, M. A.; Guyot-Sionnest, P. Bright UV-Blue Luminescent Colloidal ZnSe Nanocrystals. *J. Phys. Chem. B* **1998**, *102*, 3655−3657.
(32) Manna, L.; Scher, E. C.; Li, L. S.; Alivisatos, A. P. Epitaxial Growth and Photochemical Annealing of Graded CdS/ZnS Shells on Colloidal CdSe Nanorods. *J. Am. Chem. Soc.* **2002**, *124*, 7136−7145.
(33) Donega, C. D. Synthesis and Properties of Colloidal Heteronanocrystals. *Chem. Soc. Rev.* **2011**, *40*, 1512−1546.
(34) Ithurria, S.; Talapin, D. V. Colloidal Atomic Layer Deposition (c-ALD) Using Self-Limiting Reactions at Nanocrystal Surface Coupled to Phase Transfer between Polar and Nonpolar Media. *J. Am. Chem. Soc.* **2012**, *134*, 18585−18590.
(35) Mahler, B.; Nadal, B.; Bouet, C.; Patriarche, G.; Dubertret, B. Core/Shell Colloidal Semiconductor Nanoplatelets. *J. Am. Chem. Soc.* **2012**, *134*, 18591−18598.
(36) Nag, A.; Kovalenko, M. V.; Lee, J. S.; Liu, W. Y.; Spokoyny, B.; Talapin, D. V. Metal-free Inorganic Ligands for Colloidal Nanocrystals: S(2-), HS(−), Se(2-), HSe(−), Te(2-), HTe(−), TeS(3)(2-), OH(−), and NH(2)(−) as Surface Ligands. *J. Am. Chem. Soc.* **2011**, *133*, 10612−10620.
(37) Kovalenko, M. V.; Scheele, M.; Talapin, D. V. Colloidal Nanocrystals with Molecular Metal Chalcogenide Surface Ligands. *Science* **2009**, *324*, 1417−1420.
(38) Thomson, J. W.; Nagashima, K.; Macdonald, P. M.; Ozin, G. A. From Sulfur-Amine Solutions to Metal Sulfide Nanocrystals: Peering into the Oleylamine-Sulfur Black Box. *J. Am. Chem. Soc.* **2011**, *133*, 5036−5041.
(39) Tessier, M. D.; Mahler, B.; Nadal, B.; Heuclin, H.; Pedetti, S.; Dubertret, B. Spectroscopy of Colloidal Semiconductor Core/Shell Nanoplatelets with High Quantum Yield. *Nano Lett.* **2013**, *13*, 3321−3328.
(40) Prudnikau, A.; Chuvilin, A.; Artemyev, M. CdSe−CdS Nanoheteroplatelets with Efficient Photoexcitation of Central CdSe Region through Epitaxially Grown CdS Wings. *J. Am. Chem. Soc.* **2013**, *135*, 14476−14479.
(41) Tessier, M. D.; Spinicelli, P.; Dupont, D.; Patriarche, G.; Ithurria, S.; Dubertret, B. Efficient Exciton Concentrators Built from Colloidal Core/Crown CdSe/CdS Semiconductor Nanoplatelets. *Nano Lett.* **2014**, *14*, 207−213.
(42) Benchamekh, R.; Gippius, N. A.; Even, J.; Nestoklon, M. O.; Jancu, J. M.; Ithurria, S.; Dubertret, B.; Efros, A.; Voisin, P. Tight-binding calculations of image-charge effects in colloidal nanoscale platelets of CdSe. *Phys. Rev. B* **2014**, *89*, No. 035307.
(43) Pedetti, S.; Ithurria, S.; Heuclin, H.; Patriarche, G.; Dubertret, B. Type-II CdSe/CdTe Core/Crown Semiconductor Nanoplatelets. *J. Am. Chem. Soc.* **2014**, *136*, 16430−16438.
(44) Son, D. H.; Hughes, S. M.; Yin, Y. D.; Alivisatos, A. P. Cation Exchange Reactions-in Ionic Nanocrystals. *Science* **2004**, *306*, 1009−1012.
(45) Li, H. B.; Zanella, M.; Genovese, A.; Povia, M.; Falqui, A.; Giannini, C.; Manna, L. Sequential Cation Exchange in Nanocrystals: Preservation of Crystal Phase and Formation of Metastable Phases. *Nano Lett.* **2011**, *11*, 4964−4970.
(46) Beberwyck, B. J.; Surendranath, Y.; Alivisatos, A. P. Cation Exchange: A Versatile Tool for Nanomaterials Synthesis. *J. Phys. Chem. C* **2013**, *117*, 19759−19770.
(47) Li, H.; Brescia, R.; Krahne, R.; Bertoni, G.; Alcocer, M. J. P.; D'Andrea, C.; Scotognella, F.; Tassone, F.; Zanella, M.; De Giorgi, M.;

DOI: 10.1021/ar500326c
Acc. Chem. Res. 2015, 48, 22−30

Manna, L. Blue-UV-Emitting ZnSe(Dot)/ZnS(Rod) Core/Shell Nanocrystals Prepared from CdSe/CdS Nanocrystals by Sequential Cation Exchange. *ACS Nano* **2012**, *6*, 1637−1647.
(48) Li, H.; Brescia, R.; Povia, M.; Prato, M.; Bertoni, G.; Manna, L.; Moreels, I. Synthesis of Uniform Disk-Shaped Copper Telluride Nanocrystals and Cation Exchange to Cadmium Telluride Quantum Disks with Stable Red Emission. *J. Am. Chem. Soc.* **2013**, *135*, 12270−12278.
(49) Yang, X.; Xue, H. T.; Xu, J.; Huang, X.; Zhang, J.; Tang, Y. B.; Ng, T. W.; Kwong, H. L.; Meng, X. M.; Lee, C. S. Synthesis of Porous ZnS:Ag2S Nanosheets by Ion Exchange for Photocatalytic H-2 Generation. *ACS Appl. Mater. Interfaces* **2014**, *6*, 9078−9084.
(50) Bouet, C.; Laufer, D.; Mahler, B.; Nadal, B.; Heuclin, H.; Pedetti, S.; Patriarche, G.; Dubertret, B. Synthesis of Zinc and Lead Chalcogenide Core and Core/Shell Nanoplatelets Using Sequential Cation Exchange Reactions. *Chem. Mater.* **2014**, *26*, 3002−3008.
(51) Lesnyak, V.; George, C.; Genovese, A.; Prato, M.; Casu, A.; Ayyappan, S.; Scarpellini, A.; Manna, L. Alloyed Copper Chalcogenide Nanoplatelets via Partial Cation Exchange Reactions. *ACS Nano* **2014**, *8*, 8407−8818.
(52) Glotzer, S. C.; Solomon, M. J. Anisotropy of Building Blocks and Their Assembly into Complex Structures. *Nat. Mater.* **2007**, *6*, 557−562.
(53) Nie, Z. H.; Petukhova, A.; Kumacheva, E. Properties and Emerging Applications of Self-Assembled Structures Made from Inorganic Nanoparticles. *Nat. Nanotechnol.* **2010**, *5*, 15−25.
(54) Saunders, A. E.; Ghezelbash, A.; Smilgies, D. M.; Sigman, M. B.; Korgel, B. A. Columnar Self-Assembly of Colloidal Nanodisks. *Nano Lett.* **2006**, *6*, 2959−2963.
(55) Du, X. S.; Mo, M. S.; Zheng, R. K.; Lim, S. H.; Meng, Y. Z.; Mai, Y. W. Shape-Controlled Synthesis and Assembly of Copper Sulfide Nanoparticles. *Cryst. Growth Des.* **2008**, *8*, 2032−2035.
(56) Li, X. M.; Shen, H. B.; Niu, J. Z.; Zhang, Y. G.; Wang, H. Z.; Li, L. S. Columnar Self-Assembly of Cu_2S Hexagonal Nanoplates Induced by Tin(IV)-X Complex as Inorganic Surface Ligand. *J. Am. Chem. Soc.* **2010**, *132*, 12778−12779.
(57) Paik, T.; Ko, D. K.; Gordon, T. R.; Doan-Nguyen, V.; Murray, C. B. Studies of Liquid Crystalline Self-Assembly of GdF(3) Nanoplates by In-Plane, Out-of-Plane SAXS. *ACS Nano* **2011**, *5*, 8322−8330.
(58) Ye, X.; Chen, J.; Engel, M.; Millan, J. A.; Li, W.; Qi, L.; Xing, G.; Collins, J. E.; Kagan, C. R.; Li, J.; Glotzer, S. C.; Murray, C. B. Competition of Shape and Interaction Patchiness for Self-Assembling Nanoplates. *Nat. Chem.* **2013**, *5*, 466−473.
(59) Abécassis, B.; Tessier, M. D.; Davidson, P.; Dubertret, B. Self-Assembly of CdSe Nanoplatelets into Giant Micrometer-Scale Needles Emitting Polarized Light. *Nano Lett.* **2014**, *14*, 710−715.
(60) Lhuillier, E.; Hease, P.; Ithurria, S.; Dubertret, B. Selective Electrophoretic Deposition of CdSe Nanoplatelets. *Chem. Mater.* **2014**, *26*, 4514−4520.
(61) Tessier, M. D.; Javaux, C.; Maksimovic, I.; Loriette, V.; Dubertret, B. Spectroscopy of Single CdSe Nanoplatelets. *ACS Nano* **2012**, *6*, 6751−6758.
(62) Griffin, G. B.; Ithurria, S.; Dolzhnikov, D. S.; Linkin, A.; Talapin, D. V.; Engel, G. S. Two-Dimensional Electronic Spectroscopy of CdSe Nanoparticles at Very Low Pulse Power. *J. Chem. Phys.* **2013**, *138*, No. 014705.
(63) Guzelturk, B.; Kelestemur, Y.; Olutas, M.; Delikanli, S.; Demir, H. V. Amplified Spontaneous Emission and Lasing in Colloidal Nanoplatelets. *ACS Nano* **2014**, *8*, 6599−6605.
(64) Achtstein, A. W.; Schliwa, A.; Prudnikau, A.; Hardzei, M.; Artemyev, M. V.; Thomsen, C.; Woggon, U. Electronic Structure and Exciton-Phonon Interaction in Two-Dimensional Colloidal CdSe Nanosheets. *Nano Lett.* **2012**, *12*, 3151−3157.
(65) Kunneman, L. T.; Tessier, M. D.; Heuclin, H.; Dubertret, B.; Aulin, Y. V.; Grozema, F. C.; Schins, J. M.; Siebbeles, L. D. A. Bimolecular Auger Recombination of Electron-Hole Pairs in Two-Dimensional CdSe and CdSe/CdZnS Core/Shell Nanoplatelets. *J. Phys. Chem. Lett.* **2013**, *4*, 3574−3578.
(66) Biadala, L.; Liu, F.; Tessier, M. D.; Yakovlev, D. R.; Dubertret, B.; Bayer, M. Recombination Dynamics of Band Edge Excitons in Quasi-Two-Dimensional CdSe Nanoplatelets. *Nano Lett.* **2014**, *14*, 1134−1139.
(67) Pelton, M.; Ithurria, S.; Schaller, R. D.; Dolzhnikov, D. S.; Talapin, D. V. Carrier Cooling in Colloidal Quantum Wells. *Nano Lett.* **2012**, *12*, 6158−6163.
(68) Tessier, M. D.; Biadala, L.; Bouet, C.; Ithurria, S.; Abecassis, B.; Dubertret, B. Phonon Line Emission Revealed by Self-Assembly of Colloidal Nanoplatelets. *ACS Nano* **2013**, *7*, 3332−3340.
(69) She, C. X.; Fedin, I.; Dolzhnikov, D. S.; Demortiere, A.; Schaller, R. D.; Pelton, M.; Talapin, D. V. Low-Threshold Stimulated Emission Using Colloidal Quantum Wells. *Nano Lett.* **2014**, *14*, 2772−2777.
(70) Talapin, D. V.; Lee, J. S.; Kovalenko, M. V.; Shevchenko, E. V. Prospects of Colloidal Nanocrystals for Electronic and Optoelectronic Applications. *Chem. Rev.* **2010**, *110*, 389−458.
(71) Nag, A.; Chung, D. S.; Dolzhnikov, D. S.; Dimitrijevic, N. M.; Chattopadhyay, S.; Shibata, T.; Talapin, D. V. Effect of Metal Ions on Photoluminescence, Charge Transport, Magnetic and Catalytic Properties of All-Inorganic Colloidal Nanocrystals and Nanocrystal Solids. *J. Am. Chem. Soc.* **2012**, *134*, 13604−13615.
(72) Tang, J.; Kemp, K. W.; Hoogland, S.; Jeong, K. S.; Liu, H.; Levina, L.; Furukawa, M.; Wang, X. H.; Debnath, R.; Cha, D. K.; Chou, K. W.; Fischer, A.; Amassian, A.; Asbury, J. B.; Sargent, E. H. Colloidal-Quantum-Dot Photovoltaics Using Atomic-Ligand Passivation. *Nat. Mater.* **2011**, *10*, 765−771.
(73) Koh, W. K.; Saudari, S. R.; Fafarman, A. T.; Kagan, C. R.; Murray, C. B. Thiocyanate-Capped PbS Nanocubes: Ambipolar Transport Enables Quantum Dot Based Circuits on a Flexible Substrate. *Nano Lett.* **2011**, *11*, 4764−4767.
(74) Lhuillier, E.; Pedetti, S.; Ithurria, S.; Heuclin, H.; Nadal, B.; Robin, A.; Patriarche, G.; Lequeux, N.; Dubertret, B. Electrolyte-Gated Field Effect Transistor to Probe the Surface Defects and Morphology in Films of Thick CdSe Colloidal Nanoplatelets. *ACS Nano* **2014**, *8*, 3813−3820.
(75) Dogan, S.; Bielewicz, T.; Cai, Y. X.; Klinke, C. Field-Effect Transistors Made of Individual Colloidal PbS Nanosheets. *Appl. Phys. Lett.* **2012**, *101*, No. 073102.
(76) Lhuillier, E.; Robin, A.; Ithurria, S.; Aubin, H.; Dubertret, B. Electrolyte-Gated Colloidal Nanoplatelets-Based Phototransistor and Its Use for Bicolor Detection. *Nano Lett.* **2014**, *14*, 2715−2719.
(77) Chen, Z. Y.; Nadal, B.; Mahler, B.; Aubin, H.; Dubertret, B. Quasi-2D Colloidal Semiconductor Nanoplatelets for Narrow Electroluminescence. *Adv. Funct. Mater.* **2014**, *24*, 295−302.
(78) Yu, Q.; Cui, L. M.; Lequeux, N.; Zimmers, A.; Ulysse, C.; Rebuttini, V.; Pinna, N.; Aubin, H. In-Vacuum Projection of Nanoparticles for On-Chip Tunneling Spectroscopy. *ACS Nano* **2013**, *7*, 1487−1494.
(79) Rosencher, E.; Vinter, B. *Optoelectronic*, 2nd ed.; Dunod: Paris, 2002.

DOI: 10.1021/ar500326c
Acc. Chem. Res. 2015, 48, 22−30